Human Periodontal Stem Cells Release Specialized Proresolving Mediators and Carry Immunomodulatory and Prohealing Properties Regulated by Lipoxins

ELEONORA CIANCI,[a,b,c] ANTONIO RECCHIUTI,[c] ORIANA TRUBIANI,[b,c] FRANCESCA DIOMEDE,[b,c] MARCO MARCHISIO,[a,b] SEBASTIANO MISCIA,[a,b] ROMAIN A. COLAS,[d] JESMOND DALLI,[d] CHARLES N. SERHAN,[d] MARIO ROMANO[b,c]

Key Words. Periodontal ligament stem cells • Lipoxin A$_4$ • Immunomodulation • Lipid mediators • Regeneration

[a]Department of Medicine and Aging Science, [b]StemTeCh Group, and [c]Department of Medical, Oral and Biotechnological Sciences, "G. D'Annunzio" University of Chieti-Pescara, Chieti, Italy
[d]Center for Experimental Therapeutics and Reperfusion Injury, Harvard Institutes of Medicine, Brigham and Women's Hospital and Harvard Medical School, Boston, Massachusetts, USA

Correspondence: Mario Romano, M.D., Department of Medical, Oral and Biotechnological Sciences, "G. D'Annunzio" University of Chieti-Pescara, via Luigi Polacchi, 13, 66100 Chieti, Italy. Telephone: 39 0871-541475; E-Mail: mromano@unich.it

ABSTRACT

Unresolved inflammation and tissue destruction are underlying mechanisms of periodontitis, which is linked to dysregulated polymorphonuclear neutrophil (PMN) functions. Lipoxin A$_4$ (LXA$_4$) is a specialized proresolving lipid mediator (SPM) that dampens excessive inflammation, promotes resolution, and protects from leukocyte-mediated tissue damage. Human periodontal ligament stem cells (hPDLSCs) represent key players during tissue regeneration and may contribute to resolution of inflammation; thus, they may represent a promising tool in regenerative dentistry. In the present study, we investigated the actions of hPDLSCs on PMN apoptosis and antimicrobial functions, and determined the impact of LXA$_4$ on hPDLSCs. hPDLSCs significantly reduced apoptosis and stimulated microbicidal activity of human PMNs, via both cell-cell interactions and paracrine mechanisms. Lipid mediator metabololipidomics analysis demonstrated that hPDLSCs biosynthesize SPMs, including resolvin D1, D2, D5, and D6; protectin D1; maresins; and LXB$_4$; as well as prostaglandins D$_2$, E$_2$, and F$_{2\alpha}$. LXA$_4$ significantly enhanced proliferation, migration, and wound healing capacity of hPDLSCs through the activation of its cognate receptor ALX/FPR2, expressed on hPDLSCs. Together, these results demonstrate that hPDLSCs modulate PMN functions, and provide the first evidence that stem cells generate SPM and that the LXA$_4$-ALX/FPR2 axis regulates regenerative functions of hPDLSCs by a novel receptor-mediated mechanism. STEM CELLS TRANSLATIONAL MEDICINE 2016;5:20–32

SIGNIFICANCE

These findings uncovered unappreciated features of stem cells from the periodontal ligament, supporting the notion that these cells may act as master regulators of pathophysiological events through the release of mediators that promote the resolution of inflammation and bacterial killing. The study also demonstrated that it is possible to modulate important functions of periodontal stem cells using lipoxin A$_4$, a potent endogenous stop signal of inflammation. Thus, this study revealed an unappreciated anti-inflammatory proregenerative circuit that may be exploited to combat periodontal pathologies using resident stem cells. Moreover, the data may represent a more general template to explain the immunomodulatory functions of stem cells.

INTRODUCTION

Acute inflammation is a protective host response, which, if timely and self-limited, leads to elimination of pathogens and to homeostasis restoration [1, 2]. In oral tissues, excessive or unresolved pathogen-induced inflammation causes tissue injury and periodontitis (PD) [3, 4]. Hence, while PD etiology is bacterial, a failure to resolve inflammation is a pathophysiological determinant in PD progression [5]. PD is associated with

cardiovascular disease [6]; therefore, the need for efficacious treatment of periodontal inflammation is urgent.

Resolution of acute inflammation is an active and highly coordinated response, involving endogenous proresolving mediators, biosynthesized locally, that control leukocyte trafficking and restore homeostasis [7, 8]. Among them, specialized proresolving lipid mediators (SPMs), derived from polyunsaturated fatty acids (PUFAs), including lipoxins (LXs), resolvins (Rvs), protectins,

and maresins, perform multipronged actions that improve the outcome of inflammation-related pathologies in experimental models and clinical trials [8–11]. LXA$_4$ and its isomer 15-epi-LXA$_4$ are biosynthesized from arachidonic acid (AA) by transcellular mechanisms during inflammation resolution [12, 13]. They control polymorphonuclear neutrophil (PMN) infiltration into inflamed tissues and attract monocytes/macrophages, enhancing efferocytosis and bacterial phagocytosis, hallmarks of resolution [14]. These actions are mediated by the activation of a specific G-protein-coupled receptor (GPCR) termed ALX/FPR2 [15, 16]. LXA$_4$ is found in the gingival crevicular fluid and in peripheral blood of patients with PD [17, 18]. Moreover, SPMs combat excessive inflammation and tissue destruction in experimental PD [4]. Along these lines, LXA$_4$, 15-epi-LXA$_4$, and related synthetic stable analogs limit PMN infiltration and activation triggered by microorganisms in vitro [17, 19] and in an animal model of ligature plus infection-induced PD, improving the clinical outcome [20]. In addition, LXA$_4$ significantly reduces PD-related bone loss [20], supporting the relationship between nonresolving inflammation and tissue destruction in PD, and providing a rational approach to stimulate wound healing and tissue regeneration. Nevertheless, it is unclear whether the protective actions of LXs in PD include, in addition to anti-PMN-driven periodontal damage, the stimulation of proregenerative activities of cells in the periodontium.

Periodontal ligament (PDL), the soft connective tissue involved in teeth stability, homoeostasis, and repair [21, 22], contains a niche of multipotent stem cells [23, 24] that retain tissue regenerative capacity in adulthood [21, 22]. Human periodontal ligament stem cells (hPDLSCs) possess self-renewal and multilineage (osteo-, chondro-, odonto-, adipo-, and neurogenic) differentiation capability [24, 25]. Like bone marrow mesenchymal stem cells (BM-MSCs), hPDLSCs express mesenchymal antigens as well as cementoblastic/osteoblastic markers [23]. Because of these properties, hPDLSCs have been used in preclinical studies to assess their periodontal healing capability [26, 27]. Along these lines, the potential therapeutic applications of MSCs in regenerative medicine have been broadened by their unique immunomodulatory properties [28, 29] via cell-cell contact and/or paracrine mechanisms [30, 31]. Similarly to BM-MSCs, hPDLSCs, expanded ex vivo, possess paracrine immunosuppressive capability by inhibiting peripheral blood mononuclear cell (PBMC) proliferation [32]. Whether they also form and release proresolution mediators remains to be determined.

In the present study, we provide evidence that hPDLSCs regulate PMN functions related to inflammation resolution and bacterial killing, and demonstrate that they biosynthesize SPMs. Moreover, we show that LXA$_4$ stimulates receptor-dependent functions of hPDLSCs relevant to tissue healing. Together, these results contribute to the elucidation of novel pathways that can be exploited for stem cell-based treatment of PD.

MATERIALS AND METHODS

Ethics Statement

The protocol and informed consent to use human periodontal ligament biopsy specimens were approved by the medical ethics committee at the Medical School, "G. D'Annunzio" University of Chieti-Pescara, Italy (no. 266/17.04.14). PDL biopsy specimens were obtained from healthy subjects (ages 20–35 years) without systemic and oral diseases who signed an informed consent form before specimen collection.

hPDLSC Isolation, Culture, and Characterization

hPDLSCs were isolated according to Trubiani et al. [33]. PDL tissues were incubated with MSC basal medium supplemented with a specific bullet kit (Lonza Group, Walkersville, MD, https://www.lonza.com) at 37°C in 5% carbon dioxide (CO$_2$) for 20 days, during which cells spontaneously migrated from the explants. Stemness surface molecules and pluripotency-associated markers were evaluated, as previously described [34]. The hPDLSC phenotype was determined by flow cytometry using the following antibodies: fluorescein isothiocyanate (FITC)-conjugated CD13, CD14/FITC, phycoerythrin (PE)-conjugated CD29, CD31/FITC, peridinin chlorophyll protein (PerCP)-cyanine (Cy) 5.5-conjugated CD34, CD44/FITC, CD45/FITC, CD73/PE, CD90/FITC, CD105/PE, CD106/FITC, allophycocyanin (APC)-conjugated CD117, CD133 /PE, CD144/FITC, CD146/PE, CD166/FITC, CD326/PerCP-Cy5.5, Alexa488-conjugated human leukocyte antigen (HLA)-ABC, HLA DR/PE (BD Bioscience, Franklin Lakes, NJ, https://www.bdbiosciences.com). Pluripotent embryonic markers NANOG/PE, octamer-binding transcription factor 4 (Oct4)/PE, stage-specific embryonic antigen (SSEA4)/FITC, and (sex determining region Y)-box 2 (Sox2)/FITC were purchased from BD Bioscience. Cells were analyzed with a FACSCalibur flow cytometer (BD Bioscience), using the Cellquest (BD Bioscience) and FlowJo (Ashland, OR, http://www.flowjo.com) software. Unstained cells were the negative control.

Colony-Forming Unit-Fibroblast Assay

To assess their colony-forming unit (CFU) capability, hPDLSCs were seeded at 1×10^3 cells per 10 ml onto 100-mm culture dishes in growth medium (Lonza Group) kept at 37°C in 5% CO$_2$. After 14 days, cells were fixed with cold methanol, stained with 0.5% crystal violet, washed with distilled water, and dried. Aggregates of 50 or more cells were scored as 1 colony forming unit-fibroblast.

Osteogenic, Chondrogenic, and Adipogenic Differentiation

The formation of a mineralized bone matrix was monitored for 21 days using human MSC (hMSC) osteogenic differentiation medium (Lonza Group), as previously described [35]. Osteogenic differentiation was determined by staining mineralized deposits with Alizarin Red S (Sigma-Aldrich, Milan, Italy, https://www.sigmaaldrich.com) and by assessing the expression of osteogenic markers (i.e., alkaline phosphatase [ALP], runt-related transcription factor 2 [RUNX2], and osteopontin [OPN]) by real-time polymerase chain reaction (PCR).

To drive hPDLSC chondrogenic differentiation, cells were grown in three-dimensional (3D) cultures incubated for 21 days with chondro-inductive medium (CIM) made of high-glucose Dulbecco's modified Eagle's medium (DMEM) containing 1 μM dexamethasone, 1 μM ascorbate-2-phosphate (Sigma-Aldrich), 1% sodium pyruvate (Sigma-Aldrich), 10% insulin-transferrin-selenium 100$\times$ concentration (Thermo Fisher Scientific, Waltham, MA, https://www.thermofisher.com), and 10 ng/ml transforming growth factor (TGF)-β_3 (PeproTech, London, U.K., https://www.peprotech.com). After 3 weeks, cells were fixed, cut into 3-μm sections and stained with 1% (wt/vol) Alcian blue 8GX (Sigma-Aldrich) for histological examination. In parallel, hPDLSC monolayers were cultured in 6-well plates for 14–21 days with CIM to assess chondrogenic-related gene expression (see below) and chondrogenic matrix deposition using Alcian blue. Adipogenesis

was induced using the hMSC adipogenic differentiation medium (Lonza Group) for 4 weeks. Lipid-drop accumulation and triglyceride content were respectively evaluated by Red Oil staining and the AdipoRed assay (Lonza Group) [35]. All experiments were carried out with hPDLSCs at passages 3–7.

PMN Isolation and Coculture With hPDLSCs

PMNs were isolated from healthy volunteers (25–40 years old), who denied taking medication at least for 5 days, using dextran-histopaque sedimentation [37]. Isolated PMNs were, on average, 93% viable, as determined by flow cytometric analysis of annexin V (annV) and propidium iodide (PI) staining (annexin V-FITC Apoptosis Detection Kit; eBioscience, San Diego, CA, https://www.ebioscience.com). For coculture experiments, PMNs were incubated with hPDLSCs at different ratios (1:1, 5:1, 10:1) for 18 hours at 37°C and 5% CO_2. In some experiments, PMNs were cultured for 18 hours with hPDLSC-conditioned medium (CdM). In others, PMNs were exposed to human interleukin (IL)-8 (100 ng/ml) (PeproTech) for 30 minutes at room temperature (RT) before coculture with hPDLSCs. PMNs maintained in complete medium were used as controls.

To obtain CdM, hPDLSCs (passages 3–6) were seeded in 6-well plates at 3×10^5 cells per well in 2 ml of complete DMEM. Cells were cultured for 24, 48, and 72 hours at 37°C and 5% CO_2. At each time point, CdM was collected, centrifuged to remove cellular debris, and snap frozen at −80°C until use.

PMN Apoptosis

Apoptosis of PMNs with or without hPDLSCs or hPDLSC-CdM was evaluated by flow cytometry using annexinV and PI (eBioscience) double staining. Approximately 10^4 cellular events were acquired for each sample.

Bacterial Killing

The reference laboratory *Pseudomonas aeruginosa* strain PAO1 (ATCC 15692, ATCC, Manassas, VA, https://www.atcc.org) was grown (at 37°C overnight) on Muller-Hinton (MH) agar plates. At 24 hours before experiments were conducted, a single colony was picked up from the agar plate, inoculated in 5 ml of MH broth, and grown overnight under continuous agitation (300 rpm, 37°C). The following day, confluent PA01 was diluted (1:10) with fresh MH medium and grown for ~2 hours in a shaking incubator (300 rpm, 37°C) to midlog phase (optical density of 550 nm [OD_{550}] = 0.45 ± 0.05), corresponding to ~2×10^8 CFU/ml). Bacteria (2 ml) were opsonized (30 minutes, 37°C) with 10% AB human serum (Sigma-Aldrich), adjusted to an OD_{550} of ~0.45 with Dulbecco's phosphate buffered saline (PBS), and further diluted (1:5) with Roswell Park Memorial Institute (RPMI) medium containing 20% AB human serum. PMNs cocultured with hPDLSCs (10:1) for 18 hours were counted, washed twice with PBS, and suspended in antibiotic-free RPMI at a density of 10^6 cells per milliliter. Opsonized PA01 suspension (~3×10^7 CFU, 500 μl) was added to 500 μl of human PMNs (~6×10^5) and the mixtures were maintained in constant motion on a rotating wheel at 37°C. PA01 kept alone served as a control of maximal bacterial growth. After 90 minutes, aliquots of each mixture were removed, serially diluted with sterile PBS, and plated on MH agar to enumerate the viable CFUs. The PMN killing index was calculated as follows: [(CFU in the absence of PMN − CFU in the presence of PMN)/CFU in the absence of PMN × 100].

Multiplex Cytokines/Chemokines Analysis

The concentration of epidermal growth factor (EGF), IL-10, IL-6, IL-8, and vascular endothelial growth factor (VEGF) in 24-hour cultured hPDLSC-CdM was determined using a Milliplex human cytokines/chemokines kit (EMD Millipore, Billerica, MA, https://www.emdmillipore.com) according to the manufacturer's instructions. Briefly, 25 μl of medium was added to 25 μl of assay buffer, followed by 25 μl of antibody-coated magnetic beads incubated for 2 hours at RT during shaking. Plates were washed twice with buffer and incubated (1 hour, RT) with 25 μl of biotinylated antibodies followed by streptavidin-PE (30 minutes, RT). Plates were analyzed using a Luminex 100/200 platform (Luminex, Austin, TX, https://www.luminexcorp.com) equipped with the xPONENT 3.1 software. Standard curves for each analyte were generated using reference proteins. Analyte concentrations were determined by a five-parameter logistic curve. Analyses were carried out in duplicate and all incubation steps were performed in the dark.

Lipid Mediator Metabololipidomics

hPDLSCs were cultured in 150-mm plates with 9 ml of phenol-red free medium until 80% confluence. After treatment, medium and cells were harvested, using a scraper in 15-ml tubes, snap frozen in an acetone dry ice bath, and rapidly stored at −80°C. Two volumes of ice-cold methanol containing 500 pg of deuterium (d)-labeled d_4-LTB$_4$, d_5-LXA$_4$, d_5-RvD2, and d_4-PGE$_2$ (Cayman Chemical, Ann Arbor, MI, https://www.caymanchem.com) were then added and samples stored at 4°C for 45 minutes to allow for protein precipitation. Supernatants were collected after centrifugation (3,000 rpm, 10 minutes, 4°C) and brought to less that 10% of methanol content using nitrogen. All samples for liquid chromatography-tandem mass spectrometry (LC-MS-MS) analysis were extracted using C_{18} solid-phase extraction (SPE) columns (Waters, Milford, MA, https://www.waters.com), equilibrated with 6 ml of methanol and 12 ml of H_2O. Sample supernatants were acidified (pH ~3.5) and immediately loaded onto the SPE column. Samples were washed with 12 ml of hexane, eluted with 12 ml of methyl formate, taken to dryness, and suspended in phase (1:1 methanol to water) for LC-MS-MS analysis. The LC-MS-MS system (QTrap6500; ABSciex, Framingham, MA, https://sciex.com) equipped with an Agilent HP1100 binary pump (Agilent Technologies, Santa Clara, CA, https://www.chem.agilent.com) and an automatic injector was setup and operated, as described by Colas et al. [10]. To monitor and quantify the levels of the various lipid mediators (LMs), a multiple reaction monitoring method was developed with signature ion fragments for each molecule, also as described by Colas et al. [10].

Analysis of ALX/FPR2 Expression

Flow Cytometry

Surface and intracellular expression of ALX/FPR2 was evaluated in hPDLSCs from different donors using a monoclonal anti-ALX/FPR2 primary antibody (Aldevron, Fargo, ND, https://www.aldevron.com). Briefly, 5×10^5 cells per sample were fixed with 4% paraformaldehyde (PFA), washed, and incubated with buffer containing primary antibody for 60 minutes at 4°C. After removing the excess of primary antibody, cells were incubated with an anti-mouse FITC-conjugated secondary antibody. For intracellular staining, cells were permeabilized with FACS lysing and Perm2 solutions (BD Bioscience) before staining. Secondary antibody-matched controls were used to assess unspecific fluorescence.

Immunofluorescence and Confocal Microscopy

hPDLSCs grown on glass coverslips were fixed with 4% PFA, washed, and processed for ALX/FPR2 immunofluorescence. Cells were permeabilized with Triton X-100, neutralized with 5% skimmed milk in PBS for 30 minutes. Incubation with primary mouse anti-ALX/FPR2 antibody (Aldevron) (1:100) was followed by exposure to Alexa Fluor 488 green fluorescence conjugated goat anti-mouse (Molecular Probes; Thermo Fisher Scientific, Eugene, OR, https://www.thermofisher.com). For actin cytoskeleton and nuclei counter-staining, cells were incubated with AlexaFluor 594 conjugated phalloidin (Thermo Fisher Scientific), and TO-PRO (Thermo Fisher Scientific). Samples were analyzed using a Zeiss LSM510 META confocal system (Zeiss, Jena, Germany, www.zeiss. com) connected to an inverted Zeiss Axiovert 200 microscope equipped with a Plan Neofluor oil-immersion objective (40×/1.3 NA). Images were collected using an argon laser beam with excitation lines at 488 nm and a helium-neon source (543 nm and 665 nm).

RNA Isolation and Quantitative Real-Time PCR

hPDLSC total RNA was isolated with the RNeasy Plus Universal Mini Kit (Qiagen, Valencia, CA, https://www.qiagen.com) according to the manufacturer's instructions. Quantitative PCR for osteogenic markers and ALX/FPR2 was performed with an ABI PRISM 7900 HT Sequence Detection System (Applied Biosystems, Foster City, CA, https://www.appliedbiosystems.com). TaqMan gene expression assays (ALP, Hs01029144_m1, RUNX2, Hs00231692_m1, OPN, Hs00959010_m1, fatty acid binding protein 4 [FABP4], Hs01086177_m1, peroxisome proliferator-activated receptor γ [PPARγ], Hs01115513_m1, and ALX/FPR2 Hs00265954_m1 from Applied Biosystems; and ACAN, Hs.PT.56a.742783 and COMP, Hs. PT.58.2694031 from Integrated DNA Technologies, San Jose, CA, https://www.idtdna.com) were used according to standard protocols. Beta-2 microglobulin (B2M, Hs99999907_m1; Applied Biosystems) was used for template normalization. Duplicates were set up for each sample and the mRNA expression was analyzed by the comparative $2^{-\Delta\Delta Ct}$ relative quantification method [38].

Proliferation Assay

hPDLSCs (2×10^3 cells per well) were seeded in 96-well microplates with complete DMEM overnight at 37°C and 5% CO_2. The following day, cells were starved overnight with DMEM plus 1% fetal bovine serum (FBS), gently washed, and exposed to 0.001 to 1.0 nM LXA$_4$ (Calbiochem, San Diego, CA, https://www. merckmillipore.com/) or vehicle (0.01% ethanol maximum) diluted with 1% FBS-containing DMEM. Cells were enumerated after 24, 48, and 72 hours using trypan blue exclusion and data were expressed as proliferation index calculated as ratio between LXA$_4$- and vehicle-treated hPDLSCs. In some experiments, hPDLSCs were exposed to the ALX/FPR2 antagonist WRW4 (Calbiochem) (10 μM, 30 minutes) before LXA$_4$, and the cellular proliferation index was calculated as ratio between LXA$_4$- and WRW4-LXA$_4$ treated cells. Each condition was tested at least in triplicate and experiments were repeated three times using hPDLSCs from different donors.

In Vitro Wound Healing Assay

hPDLSCs (5×10^4 cells per well) were grown in 6-well plates in complete medium until 80% to 90% confluence and then starved overnight with DMEM plus 1% FBS. Wounds (~580 μm wide) were created by scraping the monolayers with a 200-μl pipette tip. Cell debris was removed by vigorous rinsing with PBS to avoid random reattachment. Thereafter, serum-free medium containing increasing concentrations of LXA$_4$ (0.01 to 1 nM) or vehicle (0.01% ethanol, maximum) were added to each well. hPDLSCs maintained in DMEM plus 10% FBS served as a control of maximal healing capacity. Wounds were monitored at 0, 3, 6, 24, and 48 hours using an optical microscope equipped with a digital camera (Canon, Tokyo, Japan, https://www.canon.com). Each well was photographed at three locations along the original wound boundary and wound width was quantified in three fields using ImageJ software (U.S. National Institutes of Health, Bethesda, MD, https://imagej.nih.gov/ij). To examine the involvement of the ALX/FPR2 receptor in LXA$_4$-regulated migration, wounded cells were exposed to the ALX/FPR2 antagonist WRW4 (10 μM, 30 minutes) before LXA$_4$, and wound closure was monitored at 0, 3, 6, 24, and 48 hours. Duplicates for each condition were examined.

Statistical Analysis

Data were expressed as mean $\pm$ SEM. Differences between groups were determined using the Student's t test. Differences were considered significant when $p < .05$.

RESULTS

Isolation and Characterization of hPDLSCs

hPDLSCs from PDL biopsy specimens consisted of cells with a homogeneous fibroblast-like morphology (Fig. 1A), reminiscent of other MSCs (e.g., bone marrow) [23] and capable of generating fibroblast colonies from single cells after 14 days of culture (Fig. 1B). hPDLSCs expressed specific MSC antigens, such as CD13, CD29, CD44, CD73, CD90, CD105, CD117, CD146, and CD166. Furthermore, these cells expressed the histocompatibility antigen HLA-ABC as well as markers of pluripotency (NANOG, Oct4, SSEA4, and Sox2). They stained negative for the hematopoietic markers CD14, CD31, CD34, CD45, and HLA-DR as well as for surface vascular endothelial-cadherin (CD144) and epithelial cell adhesion molecule (CD326) (Fig. 1C). Thus, hPDLSCs met the minimal criteria for being classified as MSCs [39].

To evaluate hPDLSC differentiation, we induced osteogenic; chondrogenic, and adipogenic commitment. Under osteoinductive conditions for 3 weeks, hPDLSCs produced mineralized extracellular matrix that was stained with Alizarin Red S and quantified (Fig. 1D, upper panel). Consistent with this, ALP and RUNX2 mRNA accumulated at early differentiation stages (7–14 days) to progressively decrease at 21 days when OPN was upregulated (Fig. 1D, lower panel).

After 21 days in chondrogenic conditions, the deposition of chondrogenic-like matrix was revealed by Alcian blue staining (Fig. 1E, upper panel), whereas real-time PCR showed a higher expression of chondrogenic-related genes as aggrecan (ACAN) and cartilage oligomeric matrix protein (COMP) compared with undifferentiated hPDLSCs ($p < .01$) (Fig. 1E, lower panel).

When hPDLSCs were subjected to adipogenic differentiation for 4 weeks, Oil Red O-positive lipid-droplet accumulation within cells was observed accompanied by an increase in triglyceride content compared with control cells ($p < .0001$) (Fig. 1F, upper panel). Consistent with this, hPDLSCs under adipogenic
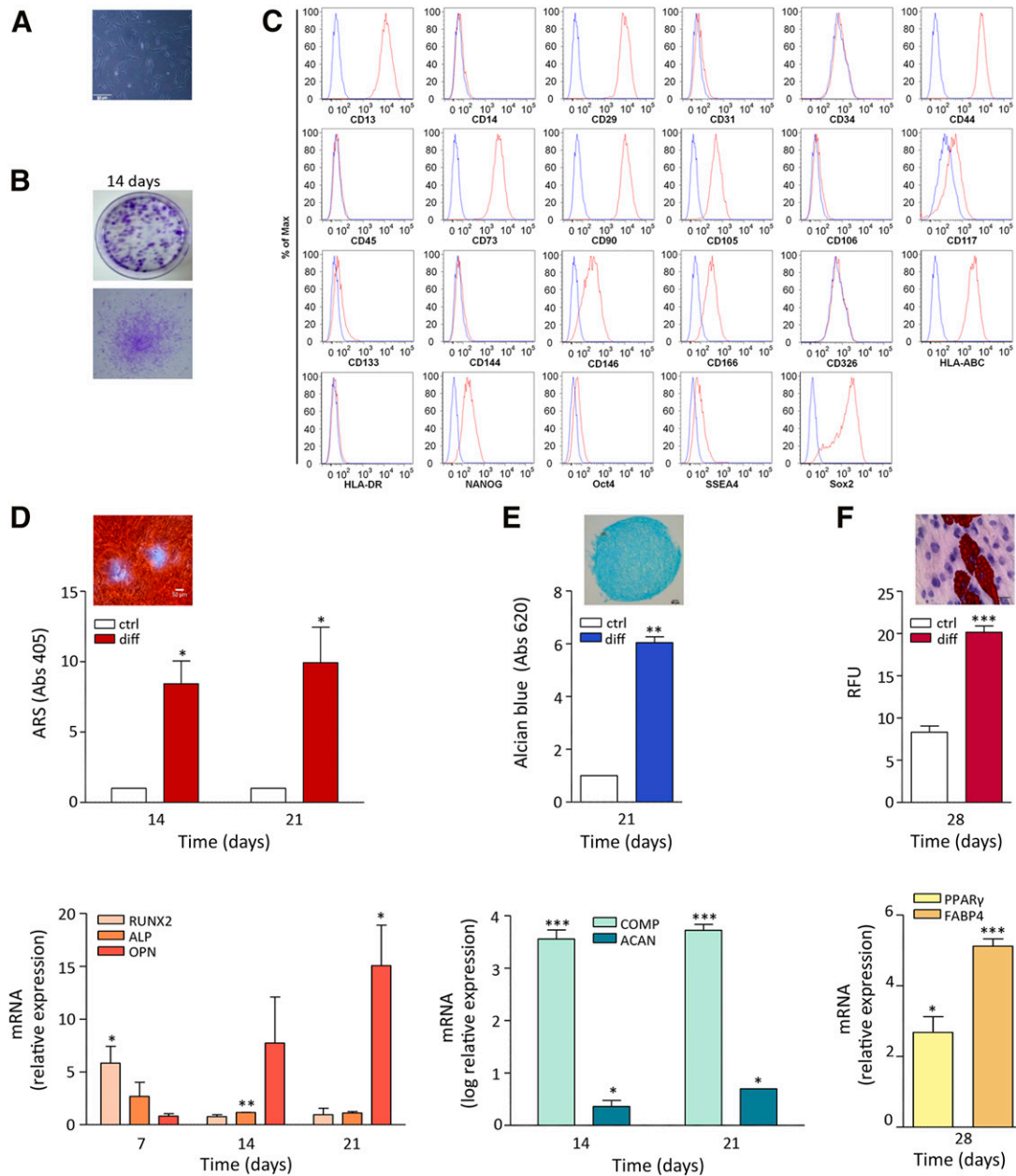
Figure 1. Human periodontal ligament stem cells (hPDLSCs) immunophenotype and differentiation. **(A):** Light microscopy image of passage-2 hPDLSCs. Original magnification: ×10. **(B):** Representative images of hPDLSC colony-forming units at 14 days. **(C):** Flow cytometric analysis of mesenchymal stem antigens in hPDLSCs. Blue histograms represent unstained cells; red histograms are stained for specific antibodies. Results are representative of five preparations. **(D):** Qualitative and quantitative analysis of hPDLSC osteogenic differentiation. Upper panel: bars represent spectrophotometric quantification of extracted ARS in control and differentiated hPDLSCs after 14 and 21 days ($n = 3$; ∗, $p < .05$). ARS-positive calcified nodules are shown in the inset (original magnification: ×10). Lower panel: mRNA evaluated by real-time polymerase chain reaction of the osteorelated genes ALP, RUNX2, and OPN at 7, 14, and 21 days of culture ($n = 3$; ∗, $p < .05$; ∗∗, $p < .01$). **(E):** Qualitative and quantitative analysis of hPDLSC chondrogenic differentiation. Upper panel: bars represent Alcian blue content in adherent hPDLSCs in normal or chondrogenic conditions at days 14 and 21 ($n = 3$; ∗∗, $p < .01$). A representative image of Alcian blue staining of chondrogenic nodules obtained from hPDLSCs after 21 days of 3-dimensional culturing is shown (inset, original magnification: ×10). Lower panel: mRNA expression of the chondrogenic-related genes ACAN and COMP at days 14 and 21 ($n = 3$; ∗, $p < .05$; ∗∗∗, $p < .001$). **(F):** Qualitative and quantitative analysis of hPDLSC adipogenic differentiation. Upper panel: bars depict the triglyceride content in hPDLSCs after 4 weeks of normal or adipogenic culturing ($n = 3$; ∗∗∗, $p < .001$). A representative image is shown of Oil Red O-positive lipid vacuoles (H&E staining for nuclei and cytoplasm). Lower panel: mRNA expression of adipogenic-related genes, such as FABP4 and PPARγ after 4 weeks of differentiation (mean ± SEM of triplicates; ∗, $p < .05$; ∗∗∗, $p < .001$). Abbreviations: abs, absorbance; ARS, Alizarin Red S; ctrl, control; diff, differentiated cells; HLA, human leukocyte antigen; OCT, octamer-binding transcription factor; RFU, relative fluorescence unit; Sox2, (sex determining region Y)-box 2; SSEA, stage-specific embryonic antigen.
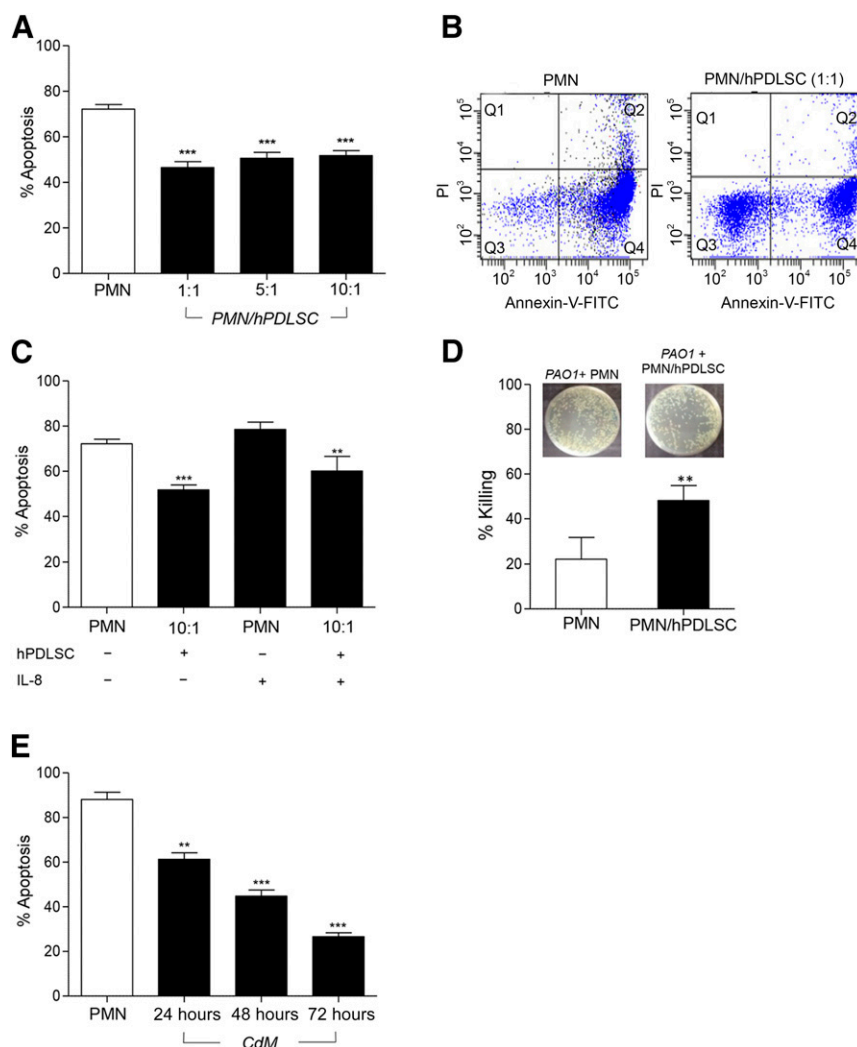
Figure 2. Effects of hPDLSCs on PMN apoptosis and bacterial killing. **(A):** PMNs were cultured with or without hPDLSCs for 18 hours. Apoptosis was evaluated by annexin V (annV)-FITC and PI staining. Results are given as the mean $\pm$ SEM of 6 independent experiments ($***$, $p < .0001$). **(B):** Representative flow cytometry dot-plot of PMNs cultured with or without hPDLSCs (1:1) for 18 hours. Lower left quadrants: viable PMNs (annV$^-$/PI$^-$); lower right quadrants: early apoptotic cells (annV$^+$); upper left quadrants: necrotic cells (PI$^+$); upper right quadrants: late apoptotic PMNs (annV$^+$/PI$^+$). **(C):** Percentage of apoptotic IL-8-activated PMNs cultured with or without hPDLSCs (1:10). Results are given as the mean $\pm$ SEM of 4 separate experiments ($**$, $p = .04$; $***$, $p < .0001$). Apoptosis is expressed as percentage of annV$^+$ cells. **(D):** PMNs cocultured with hPDLSCs for 18 hours were incubated with *Pseudomonas aeruginosa* strain PAO1 (1:50) and plated on agar. Insets show the PAO1 colony-forming units grown overnight. Results are given as the mean $\pm$ SEM of 3 experiments ($**$, $p = .0197$). **(E):** PMNs were incubated with 24-, 48- and 72-hour CdM from hPDLSCs. The percentage of apoptotic cells was evaluated by annV-FITC/PI staining. Results are given as the mean $\pm$ SEM of 4 independent experiments ($**$, $p = .0003$; $***$, $p < .0001$). Abbreviations: CdM, conditioned medium; FITC, fluorescein isothiocyanate; hPDLSC, human periodontal ligament stem cell; IL, interleukin; PI, propidium iodide; PMN, polymorphonuclear neutrophil.

culturing conditions expressed high levels of adipogenic genes as FABP4 and PPARγ compared with control cells (Fig. 1F, lower panel).

hPDLSCs Inhibit Apoptosis and Enhance Bactericidal Activity of PMNs

To evaluate the potential pathophysiological relevance of hPDLSCs in PD, we examined their impact on selected functions of PMNs, key regulators of the periodontal homeostasis [2, 40, 41]. To this end, PMNs were cocultured with hPDLSCs at different ratios for 18 hours and their survival and bactericidal activity were evaluated. hPDLSCs protected PMNs from spontaneous apoptosis ($p < .0001$), with the 1:1 ratio being most

efficient (~36% inhibition) (Fig. 2A). Also, the percentage of early apoptotic PMNs (annV$^+$/PI$^-$) was markedly reduced (from approximately ~90% to 50%; $p = .0002$) by hPDLSCs, while the percentage of viable cells (annV$^-$/PI$^-$) increased (from ~7% to 37%; $p = .0007$).

Since IL-8 drives PMN recruitment at inflammatory sites [40], we ran hPDLSC/PMN coincubations in the presence of IL-8 to mimic an inflammatory environment. Figure 2C shows that hPDLSCs also protected IL-8-activated PMNs from apoptosis, compared with PMNs treated with IL-8 alone.

To investigate whether hPDLSCs, in addition to sustaining PMN viability, maintained their bactericidal activity, we exposed PMNs from cocultures with hPDLSCs to the *P. aeruginosa* strain PAO1. PMNs derived from hPDLSC cocultures (1:10) showed higher

bactericidal activity compared with PMNs kept alone (p = .0197) (Fig. 2D), as indicated by the lower CFU number in the presence of PMNs isolated from cocultures (7.36 $\log_{10}$ ± 0.16 vs. 7.53 $\log_{10}$ ± 0.16 CFU/ml; p = .0197). Collectively, these results provide the first evidence that hPDLSCs promote survival and antibacterial activities of PMNs.

To assess whether hPDLSCs antagonized PMN apoptosis by releasing survival factors, we incubated PMNs (18 hours, 37°C) with CdM collected from hPDLSCs cultured for 24, 48, and 72 hours. As shown in Figure 2E, hPDLSC-CdM from all 3 time points significantly inhibited PMN apoptosis (p = .0003; $p < $ .0001; $p < $ .0001, respectively). Notably, 72-hour hPDLSC-CdM exhibited greater protective effect (26.61 ± 1.77 annV$^+$/PI$^-$ PMNs) compared with 48 hours (44.79 ± 2.71 annV$^+$/PI$^-$ PMNs) or 24 hours (61.33 ± 2.85 annV$^+$/PI$^-$ PMNs) CdM (Fig. 2E). Remarkably, the antiapoptotic effect of 72-hour CdM was more potent than that observed with hPDLSCs (46.50 ± 2.64 annV$^+$/PI$^-$ PMNs, 1:1 ratio) (Fig. 2A). To gain insights into this finding, we carried out multiplex cytokine analysis of hPDLSC-CdM and consistently observed that hPDLSC supernatants contain IL-6 and IL-8, which are known to inhibit PMN death [41, 42], as well as IL-10, VEGF, and EGF (Table 1). These results indicate that hPDLSCs can regulate PMN functions in a paracrine manner, producing a protective milieu that can influence resolution of inflammation and bacterial clearance.

hPDLSCs Produce SPMs

We asked whether SPM biosynthesis was a component of the immunomodulatory properties of hPDLSCs, because SPMs promote inflammation resolution and are protective in experimental PD [4]. To address this point, we performed LC-MS-MS-based LM metabololipidomics. hPDLSCs generated PUFA-derived LM from both lipoxygenase (LOX) and cyclooxygenase (COX) pathways (Fig. 3A, 3B; Table 2). In these incubations, we identified mediators from the docosahexaenoic acid (DHA)-derived bioactive metabolome including the D-series resolvins (RvD1, RvD2, RvD5, and RvD6), protectin D1 (PD1), and maresins (MaR1 and 7S,14S-diHDHA). These mediators were identified using characteristic retention times and MS-MS fragmentation in accordance with published criteria [10], as illustrated for MaR1, RvD1, and LXB$_4$ (Fig. 3B). In these hPDLSC incubations, we also identified mediators from the AA bioactive metabolome, including the LOX products LXB$_4$ and 15-epi-LXA$_4$, as well as the COX products PGD$_2$, PGE$_2$, and PGF$_{2\alpha}$. Moreover, we identified RvE2 and RvE3 from the eicosapentaenoic acid (EPA) metabolome (Fig. 3A, 3B; Table 2). These findings demonstrate that explanted hPDLSCs produce SPMs, suggesting that they may contribute to the resolution of periodontal inflammation in vivo.

LXA$_4$ Modulates the Metabolipidomic Profile of hPDLSCs

Next, we sought to determine whether proresolving mediators and receptors influenced hPDLSC activities. We focused on the ALX/FPR2-LXA$_4$ axis, which is known to improve the outcome of experimental PD [20]. hPDLSCs express ALX/FPR2 at the mRNA and protein levels, as confirmed by real-time PCR, and flow cytometry and confocal microscopy, respectively (supplemental online Fig. 1). Furthermore, ALX/FPR2 expression was not altered by cryopreservation (data not shown).

Table 1. Cytokine quantification in hPDLSC-CdM[a]

Cytokine	hPDLSC-CdM, mean ± SEM	DMEM
IL-6	199.4 ± 40.26	N.D.
IL-8	408.25 ± 241.56	N.D.
IL-10	<1.82	N.D.
EGF	1.08 ± 0.48	N.D.
VEGF	1,017.5 ± 234.88	N.D.
TNF-α	<0.06	N.D.

[a]Aliquots of hPDLSC-CdM were incubated with magnetic beads coated with antibodies specific for each cytokine for 2 hours at RT under shaking. Biotinylated detector antibodies followed by streptavidin–PE (30 min, RT) were added to the samples. Plates were analyzed using a Luminex 100/200 platform equipped with the xPONENT 3.1 software. Standard curves for each analyte were generated by using reference proteins. Analyte concentration, expressed as pg/ml, was determined with a five-parameter logistic curve. Results are given as mean ± SEM from n = 3.
Abbreviations: CdM, conditioned medium; DMEM, Dulbecco's modified Eagle's medium; EGF, epidermal growth factor; hPDLSC, human periodontal ligament stem cell; IL, interleukin; N.D., not detectable; TNF, transforming growth factor; VEGF, vascular endothelial cell growth factor.

Once ALX/FPR2 expression was demonstrated in these cells, we examined LXA$_4$ bioactions. To this end, we determined whether exposure to LXA$_4$ for 24 hours influenced the lipid mediator profile of hPDLSCs. LXA$_4$ increased D series Rvs as well as PGD$_2$, while it decreased PD1 and PGE$_2$ (Table 2). Although these changes did not reach statistical significance, because of inter-donor variability in these primary hPDLSC cultures, these results suggest that LXA$_4$ may stimulate the production of SPMs by hPDLSCs, likely triggering a proresolution feed-forward loop in the periodontium.

LXA$_4$ Stimulates ALX/FPR2-Dependent hPDLSC Proliferation and Migration

Because hPDLSCs modulate PMN activities and release mediators of inflammation and resolution, their self-renewal and migration capabilities are fundamental to achieve a pathophysiological impact. Therefore, we determined whether these functions could be modulated by LXA$_4$. hPDLSCs exposed to increasing concentrations of LXA$_4$ (0.001–1 nM) for 24, 48, and 72 hours displayed a concentration- and time-dependent increment in proliferation, with a maximum at 24 hours (Fig. 4A). This effect was suppressed by WRW4, an ALX/FPR2 antagonist peptide [44] (Fig. 4B). Likewise, LXA$_4$ concentrations as low as 0.01–1 nM significantly enhanced hPDLSC directional migration in vitro, accelerating wound closure (Fig. 5A, 5B). At 3 and 6 hours after wounding, the percentage of filled wound in LXA$_4$-treated cells was 3.5-fold higher compared with vehicle-exposed cells, and comparable to that observed in cells with 10% FBS, our control for maximal wound-healing capacity (Fig. 5A, 5B). LXA$_4$ shortened the time needed to reduce wound width by 50% (W$_{50}$) from 22 to 14 hours (~50%) (Fig. 5C). This effect was blunted by WRW4 (Fig. 5A–5C), which, instead, did not influence W$_{50}$ in cells exposed to FBS (Fig. 5D).

DISCUSSION

PD is characterized by persistent inflammation and it is associated with local and systemic morbidities [3, 6] Therefore,
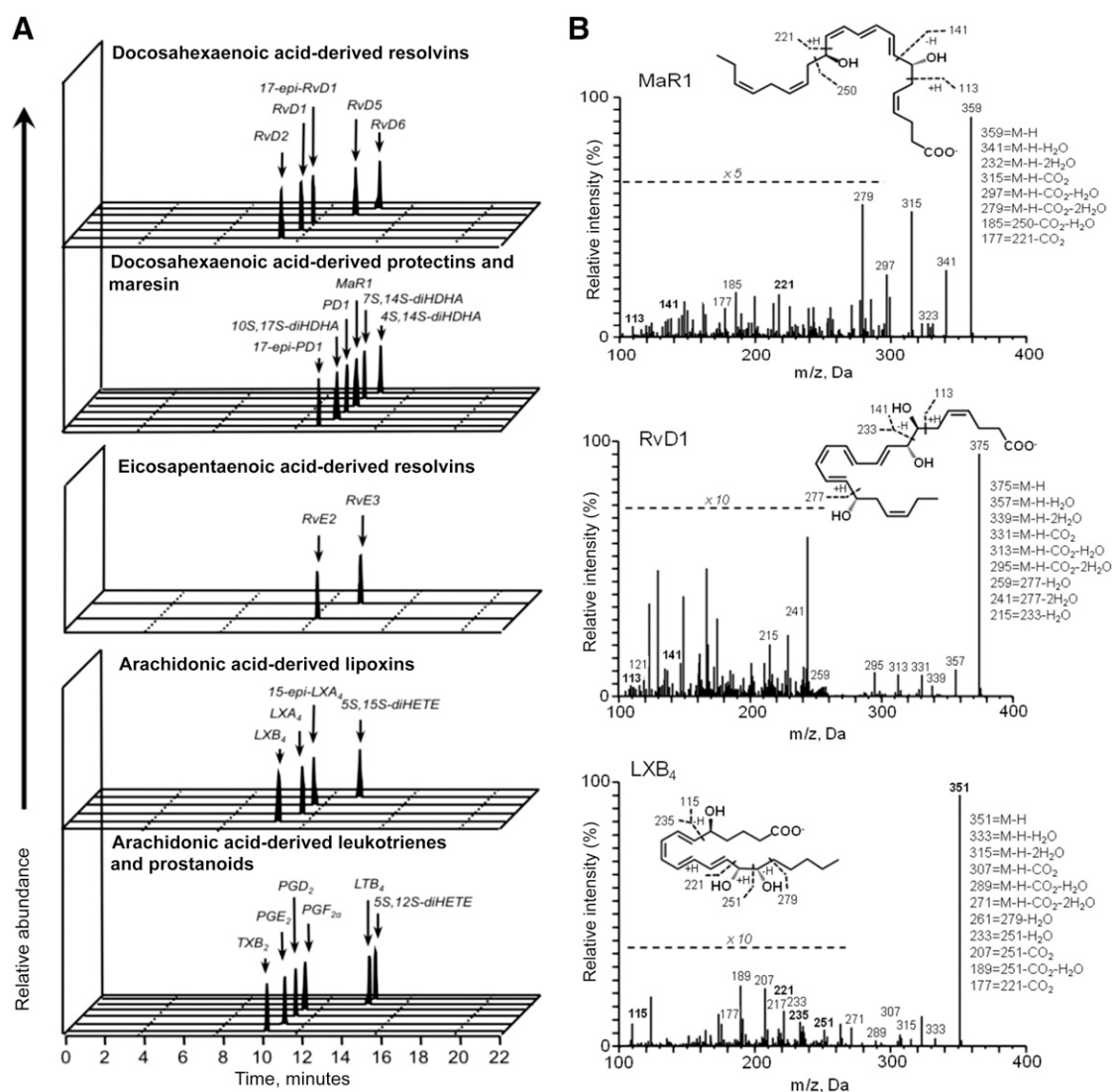
Figure 3. Bioactive lipid mediators formed by hPDLSCs. hPDLSCs were incubated for 24 hours and lipid mediators (LMs) were analyzed by LM metabololipidomics. **(A, B):** Representative multiple reaction monitoring traces, representative of seven cell preparations, for the identified LMs along with **(B)** accompanying tandem mass spectrometry spectra used for identification of MaR1, RvD1, and LXB$_4$.

knowledge of mechanisms and therapeutic approaches for this pathology is relevant for human health. In this study, we focused on stem cells isolated from the periodontal ligament. These cells have been added recently to the growing list of stem cells [23] and are likely to represent a promising tool to combat PD and related systemic consequences. hPDLSCs exhibit fibroblast-like morphology and colony-forming efficiency, and express embryonic and mesenchymal, but not hematopoietic or endothelial, markers (Fig. 1). They also express SSEA4, an embryonic marker, and the transcription factors NANOG, Oct4, and Sox2, associated with pluripotency (Fig. 1). With appropriate media, hPDLSCs differentiated into osteogenic, chondrogenic, and adipogenic lineages (Fig. 1). They can also produce cementum and PDL Sharpe's fibers [23, 45]. These properties, combined with their easy accessibility, make hPDLSCs excellent candidates for periodontal regenerative medicine.

It is widely accepted that stem cells exert immunoregulatory functions, which, in some clinical settings, represent a primary therapeutic mechanism [46]. In PD, the regulation of the host immune response is paramount for resolution [47]; PMNs are key players because they contribute to the removal of oral pathogens and tissue rebuilding [48]. Consistent with this scenario, PMN key activities, for instance chemotaxis and bacterial phagocytosis, are impaired in patients with periodontitis, thus contributing to tissue damage [40, 41].

Here, we show for the first time that hPDLSCs sustain PMN survival and bactericidal activity (Fig. 2). Cell-cell contact was not strictly necessary for these effects to take place, indicating paracrine immunoregulatory functions of hPDLSCs. Indeed, they release cytokines and growth factors (i.e., IL-8, VEGF, and IL-6) that promote PMN recruitment and survival [49, 50] (Table 1). They also release IL-10 (Table 1), which limits the proinflammatory activities of PMNs [51] and improve wound repair during PD [52]. This is consistent with a proresolutive, antimicrobial profile of the hPDLSC secretoma and prompted us to evaluate the capability of these cells to produce SPMs, pivotal regulators of inflammation resolution [8].

Table 2. Lipid mediators produced by hPDLSCs in culture: Impact of LXA$_4$[a] (n = 7 cell incubations)

Metabolome	Q1	Q3	hPDLSC LM levels (pg per 5 × 10^6 cells)		
			hPDLSC	hPDLSC + LXA$_4$ (0.1 nM)	Change, %
DHA bioactive metabolome					
RvD1	375	215	45.4	65.5	44
RvD2	375	215	60.5	95.2	57
RvD3	375	147	0.2	0.6	263
RvD5	359	199	19.7	27.2	38
RvD6	359	101	88.7	45.3	−49
17-epi-RvD1	375	215	5.3	8.7	66
17-epi-RvD3	375	147	—[b]	—[b]	NA
PD1	359	153	63.1	30.5	−52
17-epi-PD1	359	153	2.6	3.0	13
10S,17S-diHDHA	359	153	68.8	85.7	24
MaR1	359	221	11.3	11.4	1
7S,14S-diHDHA	359	221	52.4	59.7	14
4S,14S-diHDHA	359	101	50.1	65.7	31
EPA bioactive metabolome					
RvE1	349	195	—[b]	—[b]	NA
RvE2	333	213	69.2	91.9	33
RvE3	333	201	215.9	197.0	−9
AA bioacive metabolome					
LXA$_4$	351	235	0.1	—	NA
LXB$_4$	351	221	227.9	272.0	19
5S,15S-diHETE	335	235	57.0	47.3	−17
15-epi-LXA$_4$	351	115	74.6	115.6	55
15-epi-LXB$_4$	351	221			
LTB$_4$	335	195	23.7	26.5	12
5S,12S-diHETE	335	195	53.0	62.2	17
20-OH-LTB$_4$	351	195	—[b]	—[b]	NA
PGD$_2$	351	189	445.4	1,096.8	146
PGE$_2$	351	189	3,073.1	1,608.8	−48
PGF$_{2\alpha}$	353	193	123.1	70.3	−43
TxB$_2$	369	169	585.9	835.0	43

[a]Human periodontal ligament stem cells (hPDLSC) were incubated with or without 0.1 nM LXA$_4$ and LMs were assessed using LM metabololipidomics (details are available in Materials and Methods).
[b]Below the limit of detection (the detection limit was approximately 0.1 pg).
Abbreviations: —, not quantified; AA, arachidonic acid; DHA, docosahexaenoic acid; EPA, eicosapentaenoic acid; LM, lipid mediator; LXA$_4$, lipoxin A$_4$; Q1, M-H (parent ion); NA, not applicable; Q3, diagnostic ion in the tandem mass spectrometry (daughter ion).

Using an established LM metabololipidomic approach [53], we obtained the first evidence that hPDLSCs produce and release a broad spectrum of proresolutive mediators, including DHA-derived D-series resolvins, protectin D1, and maresin 1; EPA-derived resolvin E2 and E3; and AA-derived LXB$_4$ (Fig. 3). These mediators carry immunoregulatory/proresolutive bioactions by regulating granulocyte trafficking, stimulating efferocytosis and microbial clearance [8, 54]. In particular, D- and E-series resolvins regulate PMN chemotaxis and increase their capability to phagocytose and kill bacteria through specific cell-surface receptors, namely ALX/FPR2 and chemerin receptor 23 (ChemR23), widely expressed on PMNs [37, 54, 55]. Furthermore, these SPMs prevent bone resorption in experimental periodontitis [20]. hPDLSCs also produce large amounts of PGE$_2$, which regulates bone formation

and resorption [56]. Hence, hPDLSCs generate LMs that orchestrate inflammation resolution, immunomodulation, and bone metabolism.

Although it will be interesting to evaluate SPM production by stem cells from other sources, the present results provide new elements for the understanding of stem cell biology. It has been reported that stem cells exert a number of paracrine functions related to immunomodulation and control of the inflammation [28, 29]. Thus, the timely release of lipid mediators of inflammation and resolution may be regarded as a pivotal mechanism underlying these functions. Evidence that supports this hypothesis is accumulating. For instance, MSCs from umbilical cords reduce mast cell degranulation and alleviate murine atopic dermatitis through PGE$_2$ release [57]. PGE$_2$ is also key for the attenuation of graft-versus-host disease by BM-MSCs [58] and for the anti-inflammatory

effects of adipose-derived MSCs on chondrocytes and synoviocytes from osteoarthritis patients [59]. Although PGE_2 was the most abundant eicosanoid generated by hPDLSCs under routine culture conditions (Table 1), the observation, never reported before, to our knowledge, that these cells can generate SPM from DHA and EPA, which act at subnanomolar to nanomolar concentrations, suggest that: (a) the relative abundance of bioactive lipid mediators generated by stem cells could be modulated by the dietary intake of precursor fatty acids and might change in pathological conditions, and (b) the overall impact of stem cells on immuno-inflammatory responses may be dictated by a network of lipid mediators, which act in concert with peptides (Table 1).

On the other hand, the features of hPDLSCs uncovered in the present study propose these cells as key players within the context of PD, as their recruitment, proliferation, and release of proresolutive mediators can influence the outcome of PD. Here, we provide the first evidence that these processes can be modulated by an LXA_4-driven, receptor-mediated mechanism as hPDLSCs express ALX/FPR2 (supplemental online Fig. 1). In addition to LXA_4, this receptor recognizes RvD1 and annexin-A1, both carrying anti-inflammatory, proresolution functions [37]. Consistent with earlier reports showing expression of this GPCR in human BM-MSCs and its role in stem cell adhesion, migration, and homing for tissue repair [60, 61], the activation of ALX/FPR2 by LXA_4 stimulated hPDLSC proliferation and migration in vitro (Figs. 4, 5). The effect of LXA_4 on wound healing was significant already at 3 hours, ruling out the involvement of cell proliferation, at least at the earlier time points. These effects are of considerable relevance as hPDLSCs can differentiate into osteoblasts and regenerate PDL [62]; therefore, their recruitment and expansion within a diseased periodontium may accelerate tissue healing. Along these lines, LXA_4 levels are reduced in crevicular fluids and plasma from patients with PD [17, 18], thus potentially limiting endogenous hPDLSC-dependent tissue-repair mechanisms. Whether LXA_4 can trigger differentiation pathways in hPDLSCs, similar to what occurs with embryonic stem cells exposed to PD1 [63], remains to be determined.

LXA_4 also changed the LM profile of hPDLSCs (Table 2), although it did not have appreciable impact on PMN survival. Cells exposed to LXA_4, showed an increase in D-series Rvs, which control leukocyte trafficking and have antimicrobial properties in vivo [64]. LXA_4 also changed the AA metabolome: It increased PGD_2 while decreasing PGE_2 formation (Table 2). This is consistent with a proresolution profile [65]. Therefore, it appears that LXA_4 can sustain a receptor-mediated proresolution feed-forward loop that involves hPDLSCs in the periodontium.

Figure 4. ALX-FPR2-dependent stimulation of human periodontal ligament stem cell (hPDLSC) proliferation by LXA_4. **(A):** hPDLSCs were treated with LXA_4 (0.01–1 nM) or vehicle for 24, 48, and 72 hours. Proliferation was evaluated by cell count and trypan blue exclusion. Data are expressed as proliferation index (cell number with LXA_4 per cell number with vehicle) and are given as mean ± SEM from 4 independent experiments with triplicates (∗, $p < .05$ vs. vehicle). **(B):** hPDLSCs were treated with WRW4 (10 μM) before LXA_4 (0.01–0.1 nM) (∗∗, $p < .01$ WRW4 + 0.01 nM LXA_4 vs. 0.01 nM LXA_4; ∗ $p < .05$ WRW4 + 0.1 nM LXA_4 vs. 0.1 nM LXA_4). Results are given as the mean ± SEM of five experiments with triplicates. LXA_4, lipoxin A_4.

highlight the involvement of SPM and their receptors in stem cell biology, providing useful knowledge for innovative stem cell therapeutics.

CONCLUSION

The main finding of this study is that stem cells isolated from the periodontal ligament can release SPM and other mediators that carry relevant immunomodulatory, proresolution, and prohealing properties. This hPDLSC characteristic can be harnessed for therapeutic purposes in PD, although it is likely to represent a more general mechanism by which stem cells from different sources can influence the outcome of inflammatory disorders. We also demonstrate that the ALX/FPR2 receptor is crucial to promote the recruitment and expansion of hPDLSCs, thus representing a novel molecular target to enhance stem cell-mediated proresolving circuits. Collectively, these results
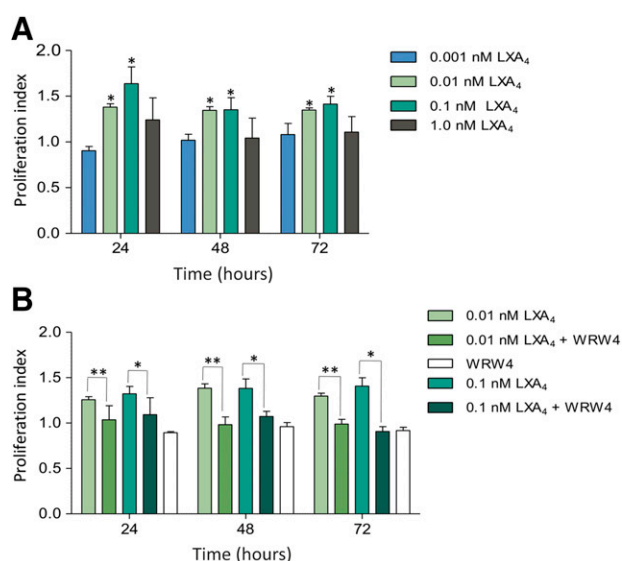
AUTHOR CONTRIBUTIONS

E.C. and A.R.: conception and design, collection and assembly of data, data analysis and interpretation, manuscript writing, final approval of manuscript; O.T.: financial support, collection and assembly of data, data analysis and interpretation, final approval of manuscript; F.D.: provision of patients, collection and assembly of data, data analysis and interpretation, final approval of manuscript; M.M.: collection and assembly of data, data analysis and interpretation, final approval of manuscript; S.M.: financial support, data analysis and interpretation, final approval of manuscript; R.A.C. and J.D.: collection and assembly of data, data analysis and interpretation, manuscript writing, final approval of manuscript; C.N.S.: data
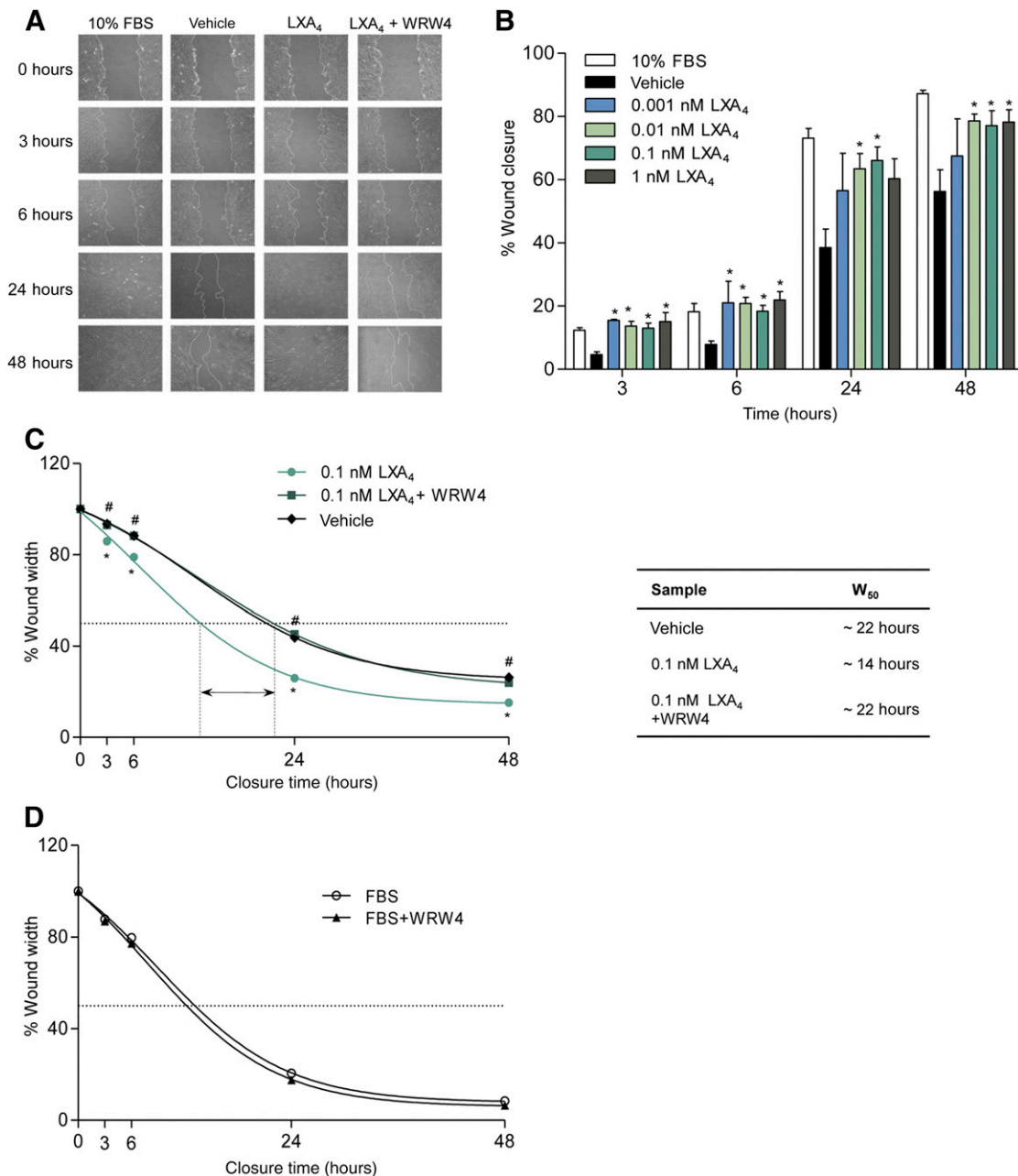
Figure 5. ALX/FPR2-dependent stimulation of human periodontal ligament stem cell (hPDLSC) migration by LXA$_4$. **(A, B):** Analysis of hPDLSC migration after exposure to LXA$_4$ (0.01–1 nM) or vehicle. Representative images of wound closure at 0, 3, 6, 24, and 48 hour (magnification: ×10) **(A)**. Wound closure was quantified at 3, 6, 24, and 48 hours postwounding, by measuring the area not filled by cells, using ImageJ software. Results are given as the mean ± SEM of percentage wound closure of 5 experiments ($*$, $p <$ .05 vs. vehicle) **(B)**. **(C):** Wounded hPDLSCs were treated with WRW4 before LXA$_4$ (0.1 nM). The arrow shows the difference (~10 hours) between time needed to reduce wound width by 50% (W$_{50}$) of LXA$_4$-treated hPDLSCs incubated with or without WRW4 ($*$, $p <$ .05 LXA$_4$ vs. vehicle; #, $p \leq$ .01 LXA$_4$ + WRW4 vs. LXA$_4$). The table displays W$_{50}$ values. **(D):** Effects of WRW4 treatment on FBS-induced migration. Results are given as the mean ± SEM of five experiments. FBS, fetal bovine serum; LXA$_4$, lipoxin A$_4$.

analysis and interpretation, manuscript writing, final approval of manuscript; M.R.: conception and design, financial support, manuscript writing, final approval of manuscript.

DISCLOSURE OF POTENTIAL CONFLICTS OF INTEREST

C.N.S. is a compensated Corbus scientific advisory board member; has compensated research funding from the NIH;

and is an uncompensated inventor on patents assigned to Brigham and Women's Hospital and Partners HealthCare on the composition of matter, uses, and clinical development of anti-inflammatory and pro-resolving lipid mediators. These include lipoxins and resolvins and related compounds that are licensed for clinical development. The resolvins are licensed to Resolvyx Pharmaceutical. The other authors indicated no potential conflicts of interest.

REFERENCES

1 Kumar V, Abbas AK, Fausto N et al. Robbins and Cotran Pathologic Basis of Disease, Professional Edition: Expert Consult-Online. St. Louis, MO: Elsevier Health Sciences, 2009.

2 Scapini P, Cassatella MA. Social networking of human neutrophils within the immune system. Blood 2014;124:710–719.

3 Pihlstrom BL, Michalowicz BS, Johnson NW. Periodontal diseases. Lancet 2005;366: 1809–1820.

4 Russell CD, Schwarze J. The role of pro-resolution lipid mediators in infectious disease. Immunology 2014;141:166–173.

5 Van Dyke TE, Serhan CN. Resolution of inflammation: A new paradigm for the pathogenesis of periodontal diseases. J Dent Res 2003;82: 82–90.

6 Holmlund A, Holm G, Lind L. Severity of periodontal disease and number of remaining teeth are related to the prevalence of myocardial infarction and hypertension in a study based on 4,254 subjects. J Periodontol 2006; 77:1173–1178.

7 Ortega-Gómez A, Perretti M, Soehnlein O. Resolution of inflammation: An integrated view. EMBO Mol Med 2013;5:661–674.

8 Serhan CN. Resolution phase of inflammation: Novel endogenous anti-inflammatory and proresolving lipid mediators and pathways. Annu Rev Immunol 2007;25:101–137.

9 Stables MJ, Gilroy DW. Old and new generation lipid mediators in acute inflammation and resolution. Prog Lipid Res 2011; 50:35–51.

10 Colas RA, Shinohara M, Dalli J et al. Identification and signature profiles for pro-resolving and inflammatory lipid mediators in human tissue. Am J Physiol Cell Physiol 2014;307: C39–C54.

11 Wu SH, Chen XQ, Liu B et al. Efficacy and safety of 15(R/S)-methyl-lipoxin A(4) in topical treatment of infantile eczema. Br J Dermatol 2013;168:172–178.

12 Serhan CN, Hamberg M, Samuelsson B. Lipoxins: Novel series of biologically active compounds formed from arachidonic acid in human leukocytes. Proc Natl Acad Sci USA 1984;81: 5335–5339.

13 Clària J, Serhan CN. Aspirin triggers previously undescribed bioactive eicosanoids by human endothelial cell-leukocyte interactions. Proc Natl Acad Sci USA 1995;92: 9475–9479.

14 Maderna P, Godson C. Lipoxins: Resolutionary road. Br J Pharmacol 2009;158:947–959.

15 Fiore S, Maddox JF, Perez HD et al. Identification of a human cDNA encoding a functional high affinity lipoxin A4 receptor. J Exp Med 1994;180:253–260.

16 Romano M, Recchia I, Recchiuti A. Lipoxin receptors. ScientificWorldJournal 2007;7:1393–1412.

17 Pouliot M, Clish CB, Petasis NA et al. Lipoxin A(4) analogues inhibit leukocyte recruitment to *Porphyromonas gingivalis*: A role for cyclooxygenase-2 and lipoxins in periodontal disease. Biochemistry 2000;39: 4761–4768.

18 Fredman G, Oh SF, Ayilavarapu S et al. Impaired phagocytosis in localized aggressive

periodontitis: rescue by Resolvin E1. PLoS One 2011;6:e24422.

19 Börgeson E, Lönn J, Bergström I et al. Lipoxin A₄ inhibits *Porphyromonas gingivalis*-induced aggregation and reactive oxygen species production by modulating neutrophil-platelet interaction and CD11b expression. Infect Immun 2011;79:1489–1497.

20 Serhan CN, Jain A, Marleau S et al. Reduced inflammation and tissue damage in transgenic rabbits overexpressing 15-lipoxygenase and endogenous anti-inflammatory lipid mediators. J Immunol 2003;171:6856–6865.

21 Bartold PM, McCulloch CA, Narayanan AS et al. Tissue engineering: a new paradigm for periodontal regeneration based on molecular and cell biology. Periodontology 2000 2000; 24:253–269.

22 Shimono M, Ishikawa T, Ishikawa H et al. Regulatory mechanisms of periodontal regeneration. Microsc Res Tech 2003;60:491–502.

23 Seo BM, Miura M, Gronthos S et al. Investigation of multipotent postnatal stem cells from human periodontal ligament. Lancet 2004; 364:149–155.

24 Lindroos B, Mäenpää K, Ylikomi T et al. Characterisation of human dental stem cells and buccal mucosa fibroblasts. Biochem Biophys Res Commun 2008;368:329–335.

25 Huang GT, Gronthos S, Shi S. Mesenchymal stem cells derived from dental tissues vs. those from other sources: Their biology and role in regenerative medicine. J Dent Res 2009;88: 792–806.

26 Sonoyama W, Liu Y, Fang D et al. Mesenchymal stem cell-mediated functional tooth regeneration in swine. PLoS One 2006;1:e79.

27 Park JY, Jeon SH, Choung PH. Efficacy of periodontal stem cell transplantation in the treatment of advanced periodontitis. Cell Transplant 2011;20:271–285.

28 Spaggiari GM, Abdelrazik H, Becchetti F et al. MSCs inhibit monocyte-derived DC maturation and function by selectively interfering with the generation of immature DCs: Central role of MSC-derived prostaglandin E2. Blood 2009;113:6576–6583.

29 Di Nicola M, Carlo-Stella C, Magni M et al. Human bone marrow stromal cells suppress T-lymphocyte proliferation induced by cellular or nonspecific mitogenic stimuli. Blood 2002; 99:3838–3843.

30 Jiang XX, Zhang Y, Liu B et al. Human mesenchymal stem cells inhibit differentiation and function of monocyte-derived dendritic cells. Blood 2005;105:4120–4126.

31 Krampera M, Glennie S, Dyson J et al. Bone marrow mesenchymal stem cells inhibit the response of naive and memory antigen-specific T cells to their cognate peptide. Blood 2003;101:3722–3729.

32 Wada N, Menicanin D, Shi S et al. Immunomodulatory properties of human periodontal ligament stem cells. J Cell Physiol 2009;219: 667–676.

33 Trubiani O, Di Primio R, Traini T et al. Morphological and cytofluorimetric analysis of adult mesenchymal stem cells expanded ex vivo from periodontal ligament. Int J Immunopathol Pharmacol 2005;18:213–221.

34 Eleuterio E, Trubiani O, Sulpizio M et al. Proteome of human stem cells from periodontal

ligament and dental pulp. PLoS One 2013;8: e71101.

35 Trubiani O, Scarano A, Orsini G et al. The performance of human periodontal ligament mesenchymal stem cells on xenogenic biomaterials. Int J Immunopathol Pharmacol 2007;20 (suppl 1):87–91.

36 Trubiani O, Piattelli A, Gatta V et al. Assessment of an efficient xeno-free culture system of human periodontal ligament stem cells. Tissue Eng Part C Methods 2015;21: 52–64.

37 Krishnamoorthy S, Recchiuti A, Chiang N et al. Resolvin D1 binds human phagocytes with evidence for proresolving receptors. Proc Natl Acad Sci USA 2010;107: 1660–1665.

38 Livak KJ, Schmittgen TD. Analysis of relative gene expression data using real-time quantitative PCR and the 2(-Delta Delta C(T)) method. Methods 2001;25: 402–408.

39 Dominici M, Le Blanc K, Mueller I et al. Minimal criteria for defining multipotent mesenchymal stromal cells. The International Society for Cellular Therapy position statement. Cytotherapy 2006;8:315–317.

40 Van Dyke TE, Horoszewicz HU, Cianciola LJ et al. Neutrophil chemotaxis dysfunction in human periodontitis. Infect Immun 1980;27: 124–132.

41 MacFarlane GD, Herzberg MC, Wolff LF et al. Refractory periodontitis associated with abnormal polymorphonuclear leukocyte phagocytosis and cigarette smoking. J Periodontol 1992;63:908–913.

42 Asensi V, Valle E, Meana A et al. In vivo interleukin-6 protects neutrophils from apoptosis in osteomyelitis. Infect Immun 2004;72: 3823–3828.

43 Kettritz R, Gaido ML, Haller H et al. Interleukin-8 delays spontaneous and tumor necrosis factor-alpha-mediated apoptosis of human neutrophils. Kidney Int 1998;53: 84–91.

44 Shin EH, Lee HY, Kim SD et al. Trp-Arg-Trp-Trp-Trp-Trp antagonizes formyl peptide receptor like 2-mediated signaling. Biochem Biophys Res Commun 2006;341:1317–1322.

45 Trubiani O, Orsini G, Zini N et al. Regenerative potential of human periodontal ligament derived stem cells on three-dimensional biomaterials: A morphological report. J Biomed Mater Res A 2008;87:986–993.

46 Weng JY, Du X, Geng SX et al. Mesenchymal stem cell as salvage treatment for refractory chronic GVHD. Bone Marrow Transplant 2010;45:1732–1740.

47 Ohlrich EJ, Cullinan MP, Seymour GJ. The immunopathogenesis of periodontal disease. Aust Dent J 2009;54(suppl 1):S2–S10.

48 Hasturk H, Kantarci A, Van Dyke TE. Oral inflammatory diseases and systemic inflammation: Role of the macrophage. Front Immunol 2012; 3:118.

49 Bickel M. The role of interleukin-8 in inflammation and mechanisms of regulation. J Periodontol 1993;64:5(suppl):456–460.

50 Sinnathamby T, Yun J, Clavet-Lanthier ME et al. VEGF and angiopoietins promote inflammatory cell recruitment and mature blood vessel formation in murine sponge/

Matrigel model. J Cell Biochem 2015;116: 45–57.

51 Bazzoni F, Tamassia N, Rossato M et al. Understanding the molecular mechanisms of the multifaceted IL-10-mediated anti-inflammatory response: lessons from neutrophils. Eur J Immunol 2010;40:2360–2368.

52 Garlet GP. Destructive and protective roles of cytokines in periodontitis: A re-appraisal from host defense and tissue destruction viewpoints. J Dent Res 2010;89: 1349–1363.

53 Lee SH, Williams MV, DuBois RN et al. Targeted lipidomics using electron capture atmospheric pressure chemical ionization mass spectrometry. Rapid Commun Mass Spectrom 2003;17:2168–2176.

54 Oh SF, Dona M, Fredman G et al. Resolvin E2 formation and impact in inflammation resolution. J Immunol 2012;188:4527–4534.

55 Herrera BS, Hasturk H, Kantarci A et al. Impact of resolvin E1 on murine neutrophil phagocytosis in type 2 diabetes. Infect Immun 2015;83:792–801.

56 Raisz LG. Physiologic and pathologic roles of prostaglandins and other eicosanoids in bone metabolism. J Nutr 1995;125:7(suppl): 2024S–2027S.

57 Kim HS, Yun JW, Shin TH et al. Human umbilical cord blood mesenchymal stem cell-derived PGE2 and TGF-β1 alleviate atopic dermatitis by reducing mast cell degranulation. Stem Cells 2015;33:1254–1266.

58 Auletta JJ, Eid SK, Wuttisarnwattana P et al. Human mesenchymal stromal cells attenuate graft-versus-host disease and maintain graft-versus-leukemia activity following experimental allogeneic bone marrow transplantation. Stem Cells 2015;33: 601–614.

59 Manferdini C, Maumus M, Gabusi E et al. Adipose-derived mesenchymal stem cells exert antiinflammatory effects on chondrocytes and synoviocytes from osteoarthritis patients through prostaglandin E2. Arthritis Rheum 2013;65:1271–1281.

60 Kim MK, Min S, Park YJ et al. Expression and functional role of formyl peptide receptor in human bone marrow-derived mesenchymal stem cells. FEBS Lett 2007;581:1917–1922.

61 Viswanathan A, Painter RG, Lanson NA Jr et al. Functional expression of N-formyl peptide receptors in human bone marrow-derived mesenchymal stem cells. Stem Cells 2007;25: 1263–1269.

62 Hoang AM, Oates TW, Cochran DL. In vitro wound healing responses to enamel matrix derivative. J Periodontol 2000;71:1270–1277.

63 Yanes O, Clark J, Wong DM et al. Metabolic oxidation regulates embryonic stem cell differentiation. Nat Chem Biol 2010;6: 411–417.

64 Spite M, Norling LV, Summers L et al. Resolvin D2 is a potent regulator of leukocytes and controls microbial sepsis. Nature 2009;461: 1287–1291.

65 Gilroy DW, Colville-Nash PR, Willis D et al. Inducible cyclooxygenase may have anti-inflammatory properties. Nat Med 1999;5: 698–701.

See www.StemCellsTM.com for supporting information available online.